



Patterns of Sedimentation from Polydispersed Turbidity Currents

Roger T. Bonnecaze; Herbert E. Huppert; John R. Lister

Proceedings: Mathematical, Physical and Engineering Sciences, Vol. 452, No. 1953
(Oct. 8, 1996), 2247-2261.

Stable URL:

<http://links.jstor.org/sici?sici=1364-5021%2819961008%29452%3A1953%3C2247%3APOSFPT%3E2.0.CO%3B2-7>

Proceedings: Mathematical, Physical and Engineering Sciences is currently published by The Royal Society.

Your use of the JSTOR archive indicates your acceptance of JSTOR's Terms and Conditions of Use, available at <http://www.jstor.org/about/terms.html>. JSTOR's Terms and Conditions of Use provides, in part, that unless you have obtained prior permission, you may not download an entire issue of a journal or multiple copies of articles, and you may use content in the JSTOR archive only for your personal, non-commercial use.

Please contact the publisher regarding any further use of this work. Publisher contact information may be obtained at <http://www.jstor.org/journals/rsl.html>.

Each copy of any part of a JSTOR transmission must contain the same copyright notice that appears on the screen or printed page of such transmission.

JSTOR is an independent not-for-profit organization dedicated to creating and preserving a digital archive of scholarly journals. For more information regarding JSTOR, please contact jstor-info@umich.edu.

Patterns of sedimentation from polydispersed turbidity currents

BY ROGER T. BONNECAZE¹, HERBERT E. HUPPERT² AND JOHN R. LISTER²

¹*Department of Chemical Engineering, The University of Texas at Austin, Austin, TX 78712-1062, USA*

²*Institute of Theoretical Geophysics, Department of Applied Mathematics and Theoretical Physics, University of Cambridge, Cambridge CB3 9EW, UK*

Particle-driven gravity currents, as exemplified by either turbidity currents in the ocean or ignimbrite flows in the atmosphere, are buoyancy-driven flows due to the suspension of dense particles in an ambient fluid. They are formed naturally from sediment-laden outflows from rivers into coastal waters, from submarine landslides along coastal shelves or as the result of volcanic eruptions. The porous rock and sand of both consolidated and unconsolidated oil-reservoirs are often derived from the sediment deposited from turbidity currents over geological time. A knowledge of the genesis of these reservoirs may provide better methods to estimate their porosity and permeability distribution, which would improve evaluation and management of these valuable resources. This paper presents a theoretical model for the dynamics and deposition of a two-dimensional particle-driven gravity current composed of a polydispersed suspension of dense particles and compares the theoretical predictions against data obtained from laboratory experiments. After developing a scaling analysis of the governing equations, we propose a simple algebraic method to compute the areal density of deposit, or mass deposited per unit area, and the distribution of particle-sizes within deposits arising from either two-dimensional or axisymmetric currents. The resulting formulae suggest an inverse method to estimate the density of deposit and the distribution of particle sizes as a function of position in a reservoir from a limited number of cores.

1. Introduction

Regardless of the price of a barrel of oil, the optimal management of oil reservoirs is a critical issue in the production of petroleum. To evaluate the viability and potential profitability of a production method, say water-flooding or hydrofracturing, computational simulations are performed on its detailed implementation in a reservoir. To perform the simulations, however, one must know the porosity and permeability throughout the reservoir. Unfortunately, especially during the initial development of an oil field, very little information is available on the porosity and permeability, except from drilling cores at a few locations in the reservoir.

Geostatistics, particularly ‘kriging’, is one method used to estimate the distribution of porosity and permeability within a reservoir from a limited number of cores (Isaaks & Srivastava 1989; Journel 1989). Kriging is the method of best linear, unbiased interpolation of data, which assumes that the property in question is statisti-

cally stationary. It should be noted that kriging does not incorporate any information about the physical processes that brought about the distribution of porosity and permeability in the first place; it is a purely statistical method based on the available data.

However, much is known about the processes that form reservoirs. The porous rock and sand of many reservoirs, such as those off the coast of Southern California, are derived from the deposits of particle-driven gravity currents, or turbidity currents (Wesser 1977). These are flows driven by the bulk density difference or buoyancy due to the suspension of dense particles in a less dense ambient fluid. Often such turbidity currents are formed and their sediment deposited as follows. Sand and silt derived from coastal erosion or from the outflow of rivers are redistributed by the action of waves and currents and accumulate on the submarine shelf along a coastline, particularly at the head of submarine canyons. Eventually, sufficient sediment accumulates on the edge of the open shelf or, more typically, at the head of an existing canyon (McGregor & Bennett 1977, 1979) for it to be unstable, and, due perhaps to a minor earthquake or large storm, some breaks away and slides down the slope at the edge of the shelf (figure 1). This submarine landslide entrains fluid, which suspends the sediment, and when it reaches the basal plain, the dense suspension spreads like a gravity current. As this turbidity current propagates, it deposits its sediment on the basal plain, reducing its buoyancy, and therefore, its rate of advance. Hence, the dynamics and deposition of the flow are coupled processes. Clay particles are also suspended during the entrainment of the fluid as the sediment slides down the slope. These very fine particles settle out last and form a relatively impermeable barrier on top of the deposit that can later trap oil that might migrate to the deposit. Multiple events of this kind, ranging from a few to hundreds, may occur at a particular site over millions of years to form the reservoir (Wesser 1977). We note that turbidity currents can be generated by mechanisms other than slumping, notably underflow from flooded rivers, but these will not be considered further here.

The deposits on the basal plain are often observed to be nearly two-dimensional, indicating that the current follows a channelled local topography, as is the case for the Black Shell turbidite in the Hatteras Abyssal Plain analysed recently by Dade & Huppert (1994). For very large flows, the deposits can form radial fans (Mutti 1992; Dade & Huppert 1995). Also, the flow down a canyon is often sufficient to erode any sediment accumulated in the thalweg, or stream channel cut into the base, and even to erode the entire bed of the canyon itself (Inman *et al.* 1976; McGregor & Bennett 1977, 1979). Erosion and entrainment of sediment during the flow along the basal plain may or may not occur depending on the magnitude of the buoyancy force and the size of the particles.

In this paper we present a model that describes the dynamics and deposition of two-dimensional and axisymmetric particle-driven gravity currents composed of polydispersed particles spreading over a horizontal surface, such as the basal plain adjacent to a coastline. The flows are assumed to be sufficiently vigorous that the suspensions are vertically well-mixed. However, we neglect entrainment in the current of both particles from the base of the flow and fluid from the ambient. Predictions of the deposition patterns from the model are successfully compared with data from laboratory experiments of two-dimensional polydispersed gravity currents. Encouraged by this successful comparison, we propose a simple algebraic method based on a scaling analysis of the governing equations to compute the areal density of deposit, or mass deposited per unit area, and the distribution of particle-sizes within a deposit

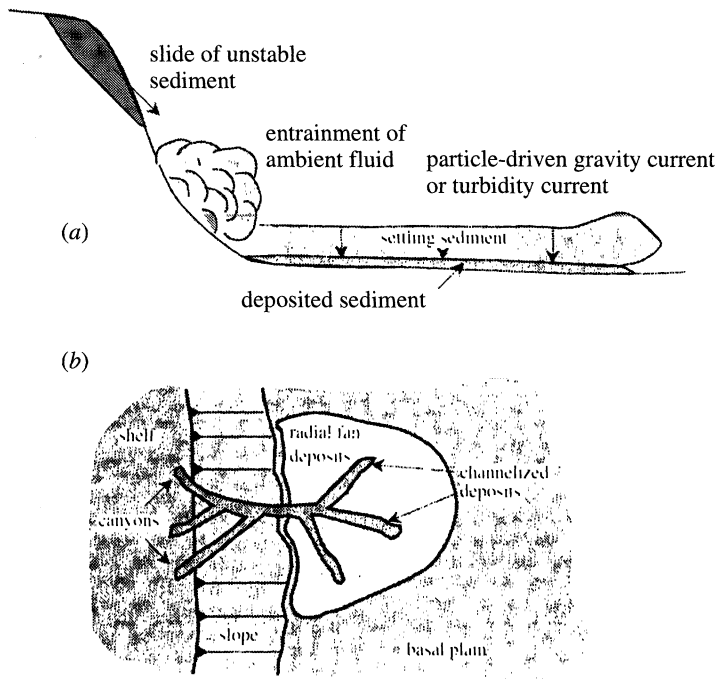


Figure 1. Schematic of the genesis of a turbidity current on a submarine shelf near a coastline and the resulting deposition patterns.

from a polydispersed turbidity current. The resulting formula suggests an inverse method using a limited number of cores to estimate the density of deposit and the distribution of particle-sizes as functions of position in a sandy reservoir emplaced by such a current. We conclude with a discussion of how these results may be used with other correlations to estimate the porosity and permeability distribution within such a reservoir.

2. Model

Bonnecaze *et al.* (1993, 1995) have developed a rigorous model for the dynamics and deposition from two-dimensional and axisymmetric particle-driven gravity currents, or turbidity currents, composed of dense particles of one size spreading over a horizontal surface. Here we extend the model to account for polydispersity of the suspended particles.

Consider a particle-driven gravity current created by the release of a fixed volume of a well-mixed suspension of bulk density ρ_c into a deep ambient body of fluid of lesser density ρ_a . The bulk density of the current, which is the local volume average of the density of particles ρ_p and the density of the interstitial fluid, here assumed to be the same as the ambient, is given by

$$\rho_c(\Phi) = (\rho_p - \rho_a)\Phi + \rho_a, \tag{2.1}$$

where Φ is the total volume fraction occupied by particles of all sizes.

The initial flow following an instantaneous release of a gravity current of finite-volume is usually complex, three-dimensional and unsteady, but quite rapidly after

initiation the current has spread sufficiently that its length $x_N(t)$ is very much greater than its height $h(x, t)$, which is a slowly varying function of the horizontal position x and time t . For such conditions, it is reasonable to neglect vertical accelerations in the flow and to assume a hydrostatic pressure distribution. We also assume that the Reynolds number of the flow is sufficiently large that viscous forces are negligible and that the dynamics of the flow are dominated by a balance between buoyancy and inertial forces. Since viscous forces are negligible, we may also assume that away from the head the horizontal velocity field $u(x, t)$ in the current is vertically uniform. These assumptions lead to the shallow-water equations, which describe conservation of mass and momentum and, for a two-dimensional turbidity current, take the form

$$\frac{\partial h}{\partial t} + \frac{\partial}{\partial x}(uh) = 0, \quad (2.2)$$

and

$$\frac{\partial}{\partial t}(uh) + \frac{\partial}{\partial x}(u^2h + \frac{1}{2}g'(\Phi)h^2) = 0, \quad (2.3)$$

where the reduced gravity $g'(\Phi) = [\rho_c(\Phi) - \rho_a]g/\rho_a$ is a function of the volume fraction of particles. We have assumed that Φ is small compared to unity and used a Boussinesq approximation which neglects $O(\Phi)$ terms in the equations of mass and momentum conservation except for the gravitational terms. In the above equations we have also assumed that the ambient fluid is very deep compared with the depth of the gravity current, so that the effects of the overlying fluid on the dynamics of the current can be neglected, and that there is negligible entrainment of the ambient fluid by the current. Effects due to entrainment are discussed by Hallworth *et al.* (1994, 1996). The effects of the overlying fluid are included by addition of mass and momentum balances for the upper layer. This has been considered in detail by Bonnecaze *et al.* (1993, 1995) for a monodispersed suspension, and the extension to a polydispersed suspension is described in Appendix A.

The particle concentration varies along the current due to advection and settling. In this paper we neglect particle entrainment into the current from the bottom over which it flows on the assumption that the slope of the bottom is sufficiently small and the fluid velocities are insufficient to lift deposited sediment into the current. We consider the flow sufficiently vigorous, however, that turbulent mixing maintains a vertically uniform particle concentration in the current, without any detrainment of particle-free fluid at the top of the current. We assume that particles of type i , which have settling velocity v_i , leave the current only through the viscous sublayer at the base with a downward flux $v_i\phi_i$, where ϕ_i denotes the volume fraction of that particle size. The equation describing the transport of each type of particle is thus

$$\frac{\partial \phi_i}{\partial t} + u \frac{\partial \phi_i}{\partial x} = -v_i \frac{\phi_i}{h}, \quad (2.4)$$

where the total volume fraction of particles $\Phi = \sum_i \phi_i$. As well as having been presented by Bonnecaze *et al.* (1993, 1995), equations similar to (2.2)–(2.4) have been derived by Garcia (1994) for a steady-state current.

The boundary conditions for equations (2.2)–(2.4) are

$$u(0, t) = 0, \quad (2.5)$$

for the case of instantaneous release of a fixed volume of suspension, and the general

condition

$$u(x_N(t), t) = Fr(g'(\Phi_N)h_N)^{1/2}, \quad (2.6)$$

where Fr is the Froude number, which relates the velocity at the front of the current to the pressure head $g'(\Phi_N)h_N$ at the front. (We use the subscript N to refer to values of the dependent variables evaluated at the nose or front of the current.) For gravity currents intruding into a deep ambient fluid with no viscous dissipation, Benjamin (1968) showed theoretically that $Fr = \sqrt{2}$, while experimentally Huppert & Simpson (1980) found a value of 1.19. The experimental value of the Froude number is somewhat lower because of viscous drag and turbulent Reynolds stresses, which cause additional momentum transfer at the head and further retard the flow of the current. These effects are only important at the three-dimensional turbulent head of the current. In addition, we must specify the initial height h_0 and length x_0 of the current and the volume fraction of particles ϕ_{i0} . Equations (2.2)–(2.6) are solved numerically with a combined finite-difference and characteristic method, which is discussed in detail by Bonneau *et al.* (1993). Note that the model has no adjustable parameters; the settling velocities of the particles are computed assuming Stokes settling and the Froude number has been determined independently by Huppert & Simpson (1980) for saline currents. Similar equations for axisymmetric particle-driven gravity currents are presented in Appendix B.

In the next section we discuss the results of some laboratory experiments against which the theoretical predictions are compared. A significant fraction of the settling in these experiments occurs when the depth of the overlying fluid is comparable to the depth of the turbidity current, which affects the velocity and depth of the current and hence the deposition. Unfortunately, it is difficult to perform experiments such that the effects of the overlying fluid can be ignored. Thus we cannot directly compare the predictions of the ‘single-layer’ model presented earlier and must, instead, augment the model to include the momentum balance of the overlying fluid, as described in Appendix A. Although this ‘two-layer’ model has the additional effect of the overlying fluid, the essential mechanisms for transport of both particles and fluid are identical. Hence, a successful comparison of the two-layer model with the experiments still validates the single-layer model as a description of the dynamics and deposition of turbidity currents in deep ambient fluids, which is more commonly the case in nature.

3. Experiments

A series of laboratory experiments were conducted to verify the predictions of the model. The experiments were performed in a glass tank 10 m long and 26 cm wide, which was filled to a height of 30 cm with tap water. A Perspex gate with foam seals around its edges was placed 15 cm from an end wall, so that the volume of fluid behind the gate was 11 700 cm³. The polydispersed suspension for the current was made by mixing various amounts of five different sizes (13, 17, 23, 37 and 53 μm diameter) of fairly monodispersed silicon carbide particles ($\rho_p = 3.217 \text{ g cm}^{-3}$) in the water behind the gate. For all the experiments reported here the initial reduced gravity of the suspensions was 22.7 cm s⁻².

The particles were well mixed in the lock, and the gate was quickly lifted to release the current. After the current had reached the end of the tank and all the particles settled, the surface density of deposit was measured along the length of the tank by the following method. A Perspex cylinder approximately 20 cm high with

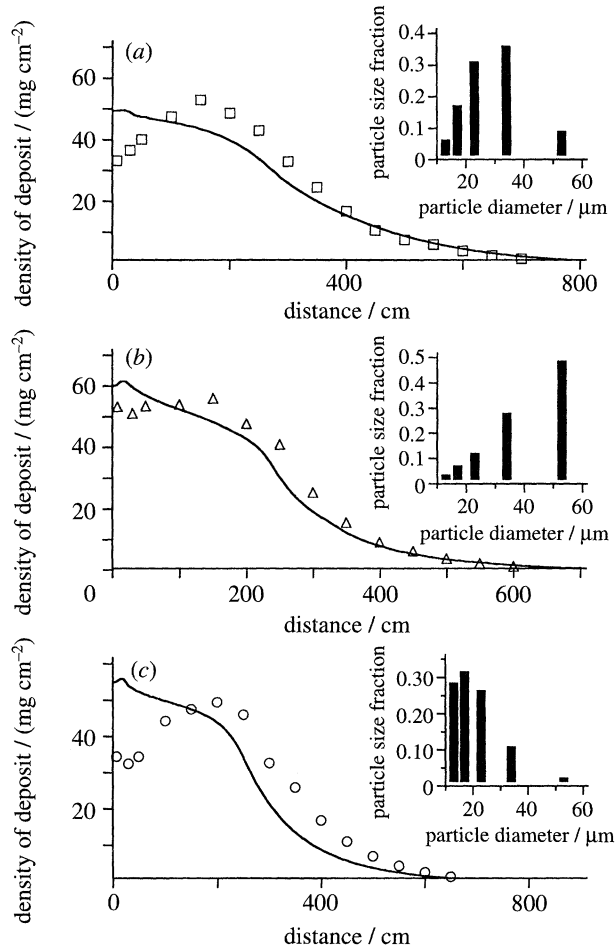


Figure 2. The experimental measurements (symbols) and theoretical predictions (lines) of the areal density of deposit for three polydispersed turbidity currents composed of silicon-carbide particles. The distribution of the five particle sizes (13, 17, 23, 37 and 53 μm) are plotted in the inset of each figure.

an internal diameter of 9.35 cm was placed vertically on the bottom of the tank at several downstream locations. All the sediment lying within it was vacuumed with a siphon tube. The particles were collected in a beaker, the water decanted and the particles dried and weighed to determine the mass per unit area.

Figure 2 presents the total density of deposit for three different particle-size distributions, which are plotted in the inset of each figure. Generally, the density of deposit decreases downstream since there are fewer particles to deposit from the current as time progresses. However, near the origin of the flow, there is a maximum in the density of deposit. This is perhaps due to particles that have already settled being transported downstream in the form of a bedload by the flow. Smaller particles are more easily transported than larger particles, causing the magnitude and position downstream of the maximum to increase with decreasing average particle size.

The theoretical predictions of the two-layer model are also plotted in figure 2. The agreement is very good, except near the origin where the model assumes that no bedload transport occurs for deposited sediment. However, the discrepancies between

theory and experiment are relatively small. Unfortunately, at this time we are unable to measure the density of deposit for each particle size to compare with the theory.

The good agreement between the theoretical predictions from our two-layer model and the experimental data gives us confidence that the single-layer model presented in §2 accurately describes the dynamics and deposition of a polydispersed gravity current spreading in a deep ambient fluid. This latter type of flow occurs often in natural settings, such as in the formation of turbidites. In the next section we develop a simple method to predict the density of deposit from a polydispersed gravity current spreading in a deep ambient fluid based on a scaling analysis of the governing equations.

4. An algebraic prediction of the density of deposit

The density of deposit, defined as the mass per unit area, is a measure of the thickness of the deposit. It would be extremely valuable to be able to determine this density and the particle-size distribution throughout a deposit, such as a sandy oil reservoir, from observations based on only a few drill-cores. Given the particle-size distribution, one could then use correlations to determine the porosity and permeability of the deposit. Specifically, we might determine values of the unknown initial conditions of the current that produced the deposit, that is, the volume fraction distributions and the initial volume of the current, by adjusting these parameters in the model (equations (2.2)–(2.6) or (A 1)–(A 6)) until the predicted deposition best matches that measured in the cores. However, this is not the most convenient method for parameter-estimation of the forward problem, since it requires repeated numerical solution of partial differential equations. Instead we propose an approximate, but much more convenient, algebraic representation of the density of deposit of each type of particle. We derive the result for a two-dimensional current here and that for an axisymmetric current in Appendix B.

For many naturally occurring turbidity flows, the depth of the turbidity current is much less than the depth of the ambient fluid, and so we may use (2.2)–(2.6) as the model equations. However, as we discuss presently, the results below are true whether the current is released in a shallow or deep ambient fluid. We commence by non-dimensionalizing equations (2.2)–(2.6) for a current composed of a monodispersed suspension. If we non-dimensionalize x by $q^{1/2}\beta_q^{-2/5}$, t by $q^{1/2}\beta_q^{2/5}/v$, h by $q^{1/2}\beta_q^{2/5}$, and u by $g_0^{1/2}q^{1/4}\beta_q^{1/5}$, where v is the settling velocity of the monodisperse particles, $q = x_0h_0$ is the initial volume per unit width of the current and $\beta_q = v/(g_0^{1/2}q^{1/4})$, equations (2.2)–(2.6) become

$$\frac{\partial \bar{h}}{\partial \bar{t}} + \frac{\partial}{\partial \bar{x}}(\bar{u}\bar{h}) = 0, \tag{4.1}$$

$$\frac{\partial}{\partial \bar{t}}(\bar{u}\bar{h}) + \frac{\partial}{\partial \bar{x}}(\bar{u}^2\bar{h} + \frac{1}{2}\Phi\bar{h}^2) = 0, \tag{4.2}$$

$$\frac{\partial \Phi}{\partial \bar{t}} + \bar{u}\frac{\partial \Phi}{\partial \bar{x}} = -\frac{\Phi}{\bar{h}}, \tag{4.3}$$

$$\bar{u}(0, \bar{t}) = 0, \tag{4.4}$$

$$\bar{u}(\bar{x}_N(\bar{t}), \bar{t}) = Fr(\Phi_N\bar{h}_N)^{1/2}, \tag{4.5}$$

where the overbarred quantities are dimensionless. In addition, the dimensionless

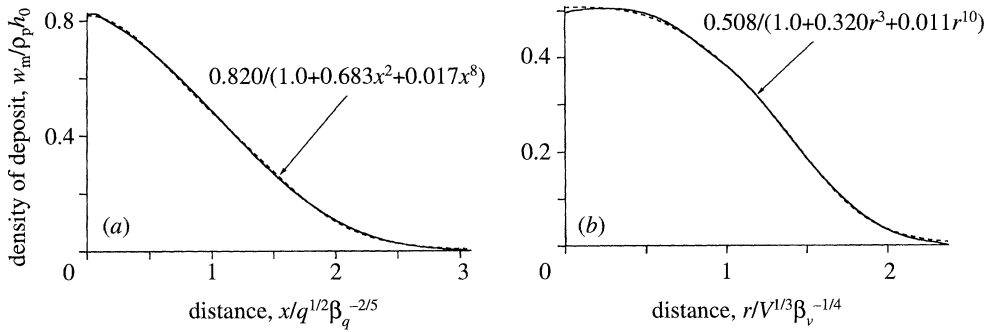


Figure 3. The dimensionless areal density of deposit for a point release of a monodispersed suspension of particles for (a) a two-dimensional turbidity current and (b) an axisymmetric turbidity current (see Appendix B). These ‘master curves’ (solid) are fitted by the algebraic functions (dashed) also illustrated on the figures.

initial conditions then become

$$\bar{h}(\bar{x}, 0) = (h_0/q^{1/2})\beta_q^{-2/5}, \tag{4.6}$$

$$\bar{x}_N(0) = (x_0/q^{1/2})\beta_q^{2/5}. \tag{4.7}$$

From this rescaling we can see that, for β_q sufficiently small that

$$(h_0/q^{1/2})\beta_q^{-2/5} \gg 1 \quad \text{and} \quad (x_0/q^{1/2})\beta_q^{2/5} \ll 1,$$

the initial shape of the suspension is essentially a delta function, and thus we expect the resulting dynamics and deposition to depend only on the initial volume and not on the details of the initial shape. One can then solve equations (7)–(13) numerically for this initial condition to compute a ‘master curve’ for the dimensionless density of deposit, $W(\bar{x})$, which is illustrated in figure 3a. The dimensional density of deposit from a monodispersed suspension is then given by $w = \rho_p q^{1/2} \Phi \beta_q^{2/5} W(\bar{x})$. A convenient and accurate empirical representation of $W(\bar{x})$ is given by

$$W(\bar{x}) = 0.820/(1 + 0.683\bar{x}^2 + 0.017\bar{x}^8). \tag{4.8}$$

These conclusions apply whether the current is released in a shallow or deep ambient fluid, provided that $(x_0/q^{1/2})\beta_q^{2/5} \ll 1$ since this condition implies that very little settling will occur until the current has spread sufficiently that its depth is much less than that of the ambient fluid. Similar conclusions have been verified for axisymmetric currents in numerical experiments by Bonnecaze *et al.* (1995).

In order to obtain a simple and rapid estimate of the density of deposit from a current composed of a polydispersed suspension of particles, we propose the following method of superposition. We assume that the dynamics and rate of propagation of the current are determined mainly by the total sediment load and volume of the current and depend only weakly on the details of the particle size distribution. As we shall see, this assumption works extremely well. By rescaling the master curve, the density of deposit w_i of particles of the i th size is thus given by

$$w_i(x) = \rho_p q^{1/2} \phi_{i0} \beta_{qi}^{2/5} W(\beta_{qi}^{2/5} x/q^{1/2}), \tag{4.9}$$

where $\beta_{qi} = v_i/(g_0^{1/2} q^{1/4})$ is the settling factor for particles of the i th size. Note that the settling factor β_{qi} which is used to scale the master curve for each particle size is defined using the *total* initial reduced gravity $g'_0 = g(\rho_p - \rho_a)\Phi/\rho_a$ based on Φ , but

the multiplying factor in the density of deposit uses only the initial volume fraction ϕ_{i0} of the i th type of particle in order to conserve mass of this species. The total density of deposit from a two-dimensional turbidity current is thus

$$w(x) = \rho_p q^{1/2} \sum_{i=1}^N \phi_{i0} \beta_{qi}^{2/5} W(\beta_{qi}^{2/5} x/q^{1/2}). \quad (4.10)$$

We tested the approximation embodied in equations (4.9)–(4.10) by comparing their predictions with those from the exact numerical solution of the single-layer model for bidispersed two-dimensional turbidity currents, which are illustrated in figure 4. The initial ratio of the mass fractions of large and small particles in the turbidity current is assumed to be unity for the test. For the large particles, the settling factor $\beta_{ql} = 10^{-3}$, and the settling factor for the small particles β_{qs} was varied such that $\beta_r = \beta_{ql}/\beta_{qs}$ ranged from 4 to 1024. This corresponds to a ratio of diameters of the large particles to the small particles ranging from 2 to 32, assuming Stokes settling in which the velocity of sedimentation is proportional to the square of the diameter of the particles. As can be seen, the agreement between the approximation and the exact numerical solution is excellent. Indeed, the difference between the two methods is practically indistinguishable.

We also tested the method for a roughly log-normal distribution of initial particle sizes in a heptadispersed current, which is illustrated in figure 5. The seven initial relative particle sizes ranged over a factor of 64, and since the Stokes settling velocity is proportional to the square of the diameter, the values of β_q ranged over a factor of 4096. The solid lines are the predictions from equations (4.9) and (4.10) and the dotted lines the exact numerical predictions. The agreement is very good. Discrepancies are only noticeable for the furthest downstream portion of the deposit and well past more than 99% of the deposit. In summary the algebraic method of superposition of the rescaled master curve provides a rapid and accurate alternative to numerical solution of the model equations for the prediction of the density of deposit of the current.

5. Conclusions and discussion

We have presented a numerical model of the dynamics and deposition of polydispersed turbidity currents and verified it by successful comparisons to laboratory experiments. In addition, in order to estimate more readily the density of a deposit from such a current, a simpler approximate algebraic method was derived from the detailed partial differential equations that describe the behaviour of a particle-driven gravity current.

Alternatively, and of great practical value for petroleum engineering, one can estimate the necessary parameters of the approximate algebraic model, namely the initial particle-size distribution and volume of the current, from a few cores and subsequently use this model to determine the density of deposit throughout sandy oil-reservoirs emplaced by turbidity currents. Our results suggest the following strategy to determine the thickness of a two-dimensional deposit from the assumed turbidity flows modeled here and the vertically averaged particle-size distribution as a function of position. We identify the density of deposit from M cores and divide the continuous distribution of particle sizes throughout the deposit into $N - 1$ discrete particle sizes, where $M \geq N$. The density and settling velocity of each discrete particle size is known, so we can estimate the N parameters, $\phi_1, \phi_2, \dots, \phi_{N-1}, q$, in equation

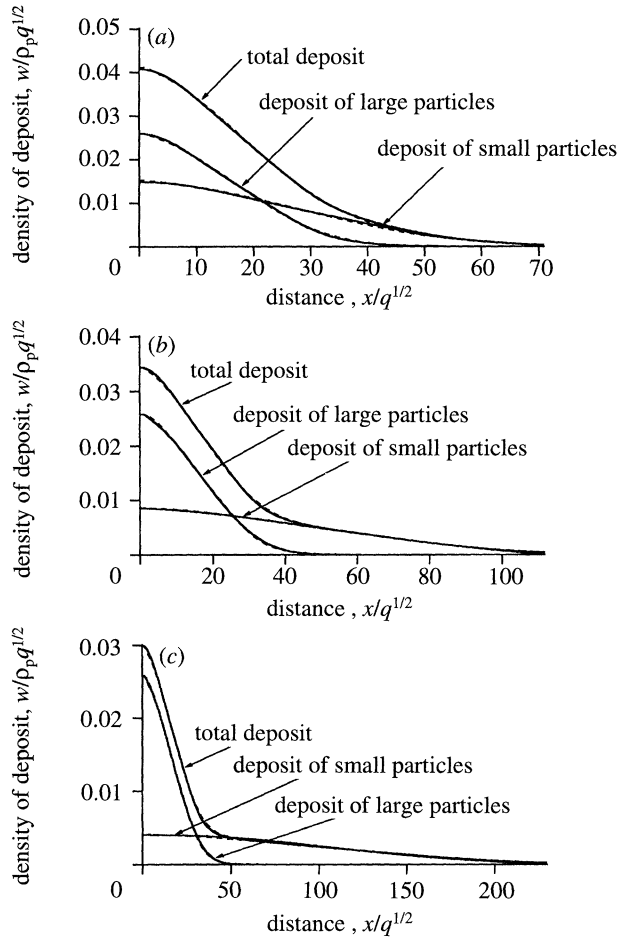


Figure 4. Comparison of the density of deposit for a bidispersed turbidity current from the full numerical solution (dashed) and the approximate algebraic method (solid) of equations (4.9) and (4.10). The initial ratio of large to small particles is unity in the suspension. The settling factor for the large particles $\beta_{ql} = 10^{-3}$ and $\beta_r = \beta_{ql}/\beta_{qs}$ is (a) 4, (b) 16, (c) 100.

(4.10) from the known density of deposit w at the M locations using, for example, an algorithm for a least-square fit to a nonlinear function. Once the parameters are determined, we can compute the density of deposit for the entire two-dimensional reservoir.

We may also determine the vertically averaged particle-size distribution as a function of position along the length of the deposit, and the vertically averaged mass-fraction of the i th particle $\chi_i = w_i/w$. Further, from available correlations, say for spherical particles (Yu & Standish 1987), we may estimate a vertically averaged porosity and convert the density of deposit into a depth of deposit, if the deposit is a sandy petroleum reservoir that has not been significantly compacted. This would be very useful for estimating the volume of oil in a newly discovered reserve from a few cores. Given the distributions of porosity and particle-sizes of the polydispersed deposit, we may also compute the permeability with available correlations (Martys *et al.* 1994), which would be valuable for feasibility studies on methods of extraction of oil from the reservoir.

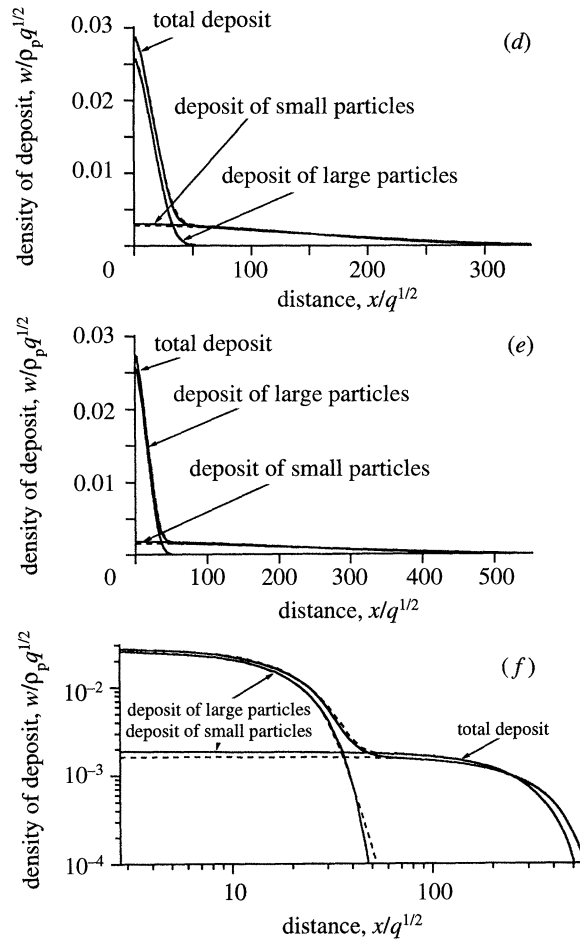


Figure 4. *Cont.* (d) 256 and (e), (f) 1024. Figure 4e is replotted on a log-log scale in (f) to see the comparison more clearly.

Of course turbidites are often subjected to secondary geological processes, such as compaction and cementation, before they become filled with oil. However, other models (Panda & Lake 1995) are available to describe these processes given inputs provided by our model. To account for the sequential application of various geological processes to determine the porosity and permeability of an oil reservoir is certainly a complex problem of nonlinear parameter estimation, but not without solution. Although our model does not describe all processes that emplace and affect the structure of turbidites, we propose here a paradigm for estimating the properties of oil reservoirs based on geophysical models.

Our model contains much more information than presented here which could be used to give a more detailed description of the properties of a turbidite. The particle-size distribution can be determined not only as a function of the extent of the deposit but also as a function of its depth. Thus, using the inverse method for the vertically averaged density of deposit, one could compute the necessary initial conditions to perform the complete numerical simulation to construct the point-wise particle-size distribution in a deposit. Again, with correlations that relate the porosity and perme-

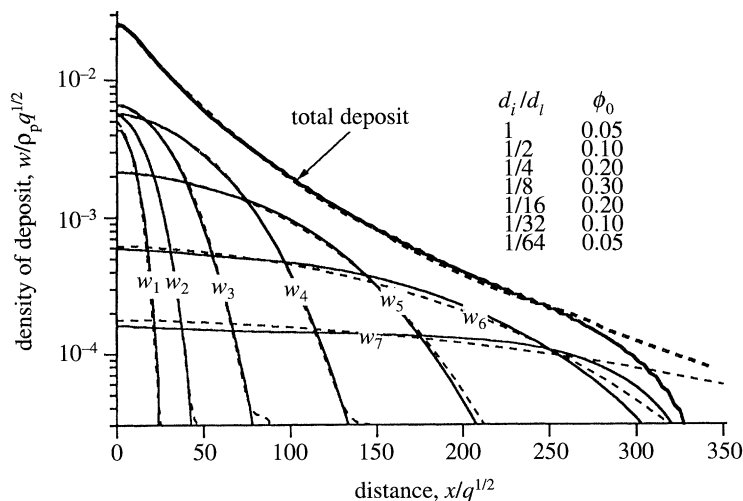


Figure 5. Areal density of deposit for a heptadispersed current computed numerically (solid lines) and with approximate method of equations (4.9) and (4.10) (dotted lines). The initial particle size distribution ϕ_0 and ratios of the particle diameters to the largest particle size, d_i/d_1 , are listed in the inset of the figure.

ability to the particle sizes and the particle-size distributions, one could construct a detailed three-dimensional map of the porosity and permeability in a deposit. These would be quite valuable for constructing simulations of petroleum reservoirs.

There are other potential applications of our model to the characterization of oil-reservoirs. Further analysis of the model may indicate how the variation of the particle-size distribution in a single core can be used to define or constrain further the properties of the reservoir. Also, for reservoirs composed of multiple turbidites, it is a common practice to describe the entire reservoir using synthetic bedding planes constrained by the few available cores (Langlais & Doyle 1992). Our method allows the construction of these synthetic bedding planes on the basis of a deterministic geophysical model, rather than some *ad hoc* statistical analysis.

Although the model for the deposition of particles has been verified by laboratory experiments, the method needs to be compared with field data. To this end we are currently searching for such data to check the approach presented here. Finally, other aspects of the dynamics and deposition of particle-driven gravity currents must also be incorporated into the model for deposition to increase its applicability. We are currently augmenting the model to include the effects of topography and of the resuspension and subsequent redeposit of particles by erosive currents.

We are grateful to W. B. Dade and two anonymous reviewers for their helpful comments on an earlier version of this manuscript. This work was partly supported by research grants from NERC.

Appendix A. Two-layer model for two-dimensional polydispersed turbidity current

When the depth of a turbidity current is comparable to the depth of the overlying fluid, a 'two-layer' model must be used to describe accurately the dynamics and resulting deposition from the current. The derivation for a monodispersed particle-

driven gravity current is described in detail by Bonnetcaze *et al.* (1993). Here we list the two-layer equations and boundary conditions for a polydispersed current.

The two-layer model is composed of the conservation of mass of the current,

$$\frac{\partial h}{\partial t} + \frac{\partial}{\partial x}(uh) = 0, \tag{A1}$$

the two-layer conservation of momentum,

$$\frac{\partial}{\partial t}(uh) + \left(1 - \frac{h}{H}\right) \frac{\partial}{\partial x} [u^2h + \frac{1}{2}g'(\Phi)h^2] + \frac{h}{H} \frac{\partial}{\partial x} [u^2h^2(H-h)^{-1}] = 0, \tag{A2}$$

and the conservation of each type of particle,

$$\frac{\partial \phi_i}{\partial t} + u \frac{\partial \phi_i}{\partial x} = -v_i \frac{\phi_i}{h}, \tag{A3}$$

where H is the combined depth of the current and overlying fluid. Equation (A2) is derived from a linear combination of the momentum balances of each layer and use of the fact that

$$u(x,t)h(x,t) + u_u(x,t)h_u(x,t) = 0, \tag{A4}$$

where u_u and h_u are the velocity and depth of the the overlying fluid, since there is no flow at $x = 0$ for the release of a fixed volume of suspension.

In addition to the no flow boundary condition $u(0,t) = 0$, there is the Froude condition at the nose of the current,

$$u(x_N(t), t) = Fr(g'(\Phi_N)h_N)^{1/2}. \tag{A5}$$

For currents intruding into relatively shallow surroundings the Froude number Fr varies with the ratio of the depth of the gravity current to the depth of the ambient fluid. Experimentally, Huppert & Simpson (1980) found that

$$\begin{aligned} Fr &= 1.19 && (0 \leq h_N/H \leq 0.075), \\ &= 0.5(H/h_N)^{1/3} && (0.075 \leq h_N/H \leq 1). \end{aligned} \tag{A6}$$

For the case of a release of a fixed volume of dense fluid whose initial depth is close to that of the ambient fluid, a two-layer hydraulic jump forms shortly after initiation of the flow. As discussed by Bonnetcaze *et al.* (1993), this alters the structure of the current and significantly changes the deposition pattern compared to that predicted by the single-layer model. However, note that the two models have the same equations to describe transport of particles. Since equations (A1)–(A3) and (A5)–(A6) reduce to equations (2.2)–(2.6) in the limit of $h/H \ll 1$, it is reasonable to assume that successful comparison of the two-layer model to experiments where the overlying fluid is of comparable depth to that of the current validates the single-layer model for currents intruding into deep ambient fluids.

Appendix B. Deposition from an axisymmetric turbidity current

The dynamics and deposition for an axisymmetric gravity current composed of a polydispersed suspension are described by the equations (Bonnetcaze *et al.* 1995)

$$\frac{\partial h}{\partial t} + \frac{1}{r} \frac{\partial}{\partial r}(ruh) = 0, \tag{B1}$$

$$\frac{\partial}{\partial t}(uh) + \frac{1}{r} \frac{\partial}{\partial r}(ru^2h) + \frac{\partial}{\partial r}(\frac{1}{2}g'(\Phi)h^2) = 0, \quad (\text{B } 2)$$

$$\frac{\partial \phi_i}{\partial t} + u \frac{\partial \phi_i}{\partial r} = -v_i \frac{\phi_i}{h}, \quad (\text{B } 3)$$

where r is the radial distance. The boundary conditions for equations (B1)–(B3) are given by equations (2.5) and (2.6), as in the case for a two-dimensional gravity current.

To determine the equations that describe the master curve for deposition from an axisymmetric particle-driven gravity current, we non-dimensionalize

$$r \text{ by } V^{1/3}\beta_V^{-1/4}, \quad t \text{ by } V^{1/3}\beta_V^{1/4}/v,$$

$$h \text{ by } V^{1/3}\beta_V^{1/4}, \quad u \text{ by } g_0^{1/2}V^{1/6}\beta_V^{1/8},$$

where V is the initial volume of the current and $\beta_V = v/(g_0^{1/2}V^{1/6})$. In non-dimensional form equations (B1)–(B3) and their boundary conditions become

$$\frac{\partial \bar{h}}{\partial \bar{t}} + \frac{1}{\bar{r}} \frac{\partial}{\partial \bar{r}}(\bar{r}\bar{u}\bar{h}) = 0, \quad (\text{B } 4)$$

$$\frac{\partial}{\partial \bar{t}}(\bar{u}\bar{h}) + \frac{1}{\bar{r}} \frac{\partial}{\partial \bar{r}}(\bar{r}\bar{u}^2\bar{h}) + \frac{\partial}{\partial \bar{r}}(\frac{1}{2}g'(\Phi)\bar{h}^2) = 0, \quad (\text{B } 5)$$

$$\frac{\partial \phi_i}{\partial \bar{t}} + \bar{u} \frac{\partial \phi_i}{\partial \bar{r}} = -v_i \frac{\phi_i}{\bar{h}}, \quad (\text{B } 6)$$

$$\bar{h}(\bar{r}, 0) = (h_0/V^{1/3})\beta_V^{-1/4}, \quad (\text{B } 7)$$

$$\bar{r}_N(0) = (r_0/V^{1/3})\beta_V^{1/4}, \quad (\text{B } 8)$$

where the overbarred quantities are dimensionless, r_0 is the initial radius of the current and $r_N(t)$ is the radius of the current. As for the case of a two-dimensional particle-driven gravity current, for β_V sufficiently small that $(h_0/V^{1/3})\beta_V^{-1/4} \gg 1$ and $(r_0/V^{1/4})\beta_V^{1/4} \ll 1$, the dynamics and deposition of the current are practically independent of its initial shape. Thus, one can solve equations (B4)–(B8) numerically, on the assumption that the initial shape of the current is a delta function, to compute the dimensionless density of deposit $W(\bar{r})$, which is shown in figure 3*b* and can be conveniently fitted by the empirical function

$$W(\bar{r}) = 0.508/(1 + 0.320\bar{r}^3 + 0.011\bar{r}^{10}). \quad (\text{B } 9)$$

The dimensional density of deposit from a monodispersed axisymmetric current is $w = \rho_p V^{1/3} \Phi \beta_V^{1/4} W(\bar{r})$.

Following the method discussed in §4, the density of deposit of particles of size i from a polydispersed axisymmetric particle-driven gravity current is then given by

$$w_i(r) = \rho_p V^{1/3} \phi_{i0} \beta_{V_i}^{1/2} W(\beta_{V_i}^{1/4} r/V^{1/3}), \quad (\text{B } 10)$$

and the total deposit is

$$w(r) = \rho_p V^{1/3} \sum_{i=1}^N \phi_{i0} \beta_{V_i}^{1/2} W(\beta_{V_i}^{1/4} r/V^{1/3}), \quad (\text{B } 11)$$

where $\beta_{V_i} = v_i/(g_0^{1/2}V^{1/6})$.

References

- Benjamin, T. B. 1968 Gravity currents and related phenomena. *J. Fluid Mech.* **88**, 223–240.
- Bonnetcaze, R. T., Huppert, H. E. & Lister, J. R. 1993 Particle-driven gravity currents. *J. Fluid Mech.* **250**, 339–369.
- Bonnetcaze, R. T., Hallworth, M. A., Huppert, H. E. & Lister, J. R. 1995 Axisymmetric particle-driven gravity currents. *J. Fluid Mech.* **294**, 93–121.
- Dade, W. B. & Huppert, H. E. 1994 Predicting the geometry of channelized deep-sea turbidites. *Geology* **22** 645–648.
- Dade, W. B. & Huppert, H. E. 1995 Runout and fine-sediment deposits of axisymmetric gravity currents. *J. Geophys. Res. (Oceans)* **100**, 18 597–18 609.
- Garcia, M. 1994 Depositional turbidity currents laden with poorly sorted sediment. *J. Hydr. Engng* **120**, 1240–1263.
- Hallworth, M. A., Phillips, J. C., Huppert, H. E. & Sparks, R. S. J. S. 1994 Entrainment in turbulent gravity currents. *Nature* **362**, 829–831.
- Hallworth, M. A., Huppert, H. E., Phillips, J. C. & Sparks, R. S. J. S. 1996 Entrainment into two-dimensional and axisymmetric turbulent gravity currents. *J. Fluid Mech.* **308**, 289–311.
- Huppert, H. E. & Simpson, J. E. 1980 The slumping of gravity currents. *J. Fluid Mech.* **90**, 785–799.
- Inman, D. L., Nordstrom, C. E. & Flick, R. E. 1976 Currents in submarine canyons: an air–sea–land interaction. *A. Rev. Fluid Mech.* **8**, 275–3109.
- Isaaks, E. H. & Srivastava, R. M. 1989 *An introduction to applied geostatistics*. New York: Oxford University Press.
- Journel, A. G. 1989 The fundamentals of geostatistics in five lessons. *Int. Geolog. Cong. Short Course in Geology*, vol. 8. American Geophysical Union.
- Langlais, V. & Doyle, J. 1992 Comparison of several methods of lithofacies simulation on the fluvial gypsy sandstone of Oklahoma. *Geostatistics Troia 92* **1**, 299–310.
- Martys, N. S., Torquato, S. & Bentz, D. P. 1994 Universal scaling of fluid permeability for sphere packings. *Phys. Rev. E* **50**, 403–408.
- McGregor, B. A. & Bennett, R. H. 1977 Continental slope instability north-east of Wilmington Canyon. *Bull. Am. Ass. Petrol. Geol.* **61**, 918–928.
- McGregor, B. A. & Bennett, R. H. 1979 Mass movement of sediment on the continental slope and rise seaward of the Baltimore Canyon trough. *Marine Geology* **33**, 163–174.
- Mutti, E. 1992 *Turbidite sandstones* **75**, Istituto di Geologia, Università di Parma.
- Perrodon, A. 1985 Dynamics of oil and gas accumulation. *Bulletin des Centres Recherches Exploration-Production*, pp. 98–105. Elf-Aquitaine, Pau, France.
- Panda, M. N. & Lake, L. W. 1995 A physical model of cementation and its effects on single-phase permeability. *AAPG Bull.* **79**, 431–443.
- Wesser, O. E. 1977 Deep-water oil sand reservoirs – ancient case histories and modern concepts. In *AAPG Continuing Education Course Notes Series 6*.
- Yu, A. B. & Standish, N. 1987 Porosity calculations of multicomponent mixtures of spherical particles. *Powder Technology* **52**, 233–241.

Received 9 June 1995; revised 31 August 1995; accepted 18 September 1995